Emergent quantum phases and excitations of bosonic atoms in an optical lattice

Philip Russ

December 2012

Bosonic atoms in an optical lattice are a useful tool for understanding strongly-interacting systems. This paper presents some of the basic theory for this system and calculations have been performed to reveal some of the properties of each phase. To compliment theory, important experimental research is highlighted which pioneered this area of study in AMO physics, including the observation of a quantum phase transition, fundamental properties of each quantum phase and excitations of the system.

Introduction

An intense area of research in modern condensed matter physics is the behavior of strongly-interacting systems at low temperatures. Perhaps the most actively studied are the high-Tc superconductors, where the electron pairing mechanism responsible for phases transitions to the superconducting state at critical temperatures in excess of 130 K has yet to be fully identified and understood. One model that has received a fair share of attention from physicists is the Hubbard model since it is thought to be able to yield the correct phase diagram of these materials. The Hubbard model describes particles on a lattice using second quantization language in the form of fermion field operators and is represented as a Hamiltonian containing the particle tunneling energy to neighboring lattice sites and the interaction energy between particles. It can be considered an improvement on traditional band theory since it is able to predict the existence of an insulating state mediated by interactions, the so-called Mott insulator, but the full phase diagram is not yet known since the strong interactions greatly increase the complexity of solving the Hamiltonian with a large number of particles and lattice sites using theory or computational methods.

Instead of fermions, we can model bosonic particles in a lattice by using boson field operators in what is known as the Bose-Hubbard model. This is relevant for understanding the behaviour of certain traditionally condensed matter systems like superfluid He-4 in disordered media. In this paper, we will discuss the physics of bosonic atoms in a three-dimensional optical lattice at ultracold temperatures, a system which is an ideal realization of the Bose-Hubbard model. Ultracold atomic systems like this are highly advantageous for studying Hubbard models due to the experimentalist's ability to tune the system parameters with a knob and map the phase diagram through measurements of the gas density profile. For the work discussed here, this atomic system is being used as a quantum simulator, a highly-controllable quantum system whose low-level physics we understand and behavior is similar to the system of interest. Drawing comparisons to solids, this quantum simulator employs atoms as electrons and the optical lattice potential formed by standing electromagnetic waves as a crystal lattice. Atoms can move between minima in the standing wave potential via tunneling just as electrons can move between lattice sites in the crystal while atom-atom interactions take the place of Coulomb interactions between electrons.

An optical lattice is produced by interfering pairs of counter-propagating laser beams to form a standing wave in three mutually orthogonal directions. The potential formed by this setup is given by:

$$V = V_0 \sum_{i=1}^{3} \sin^2(k_i x_i) \tag{1}$$

where k_i are the lattice laser wavenumbers along each of the orthogonal directions. The variable V_0 is the lattice depth and depends on the frequency of the atomic transition, the frequency and polarization of the laser and the spin state of the atom. It is common to measure the lattice depth in units of the recoil energy $E_R = \frac{\hbar^2|\vec{k}|^2}{2m}$, where $\vec{k}$ is the wavevector of the laser and m is the mass of the atom. The wavenumbers are usually quite close to equal in each direction so a good approximation is that we have a cubic lattice as far as the precision of our measurements is concerned. Atoms are first cooled to quantum degeneracy

and loaded into an optical lattice from a magnetic or optical trap by slowly increasing the laser power at the atomic cloud. The dispersion relation is modified by the presence of this periodic potential and instead of the typical $E \propto |\vec{k}|^2$ for a free particle, the energy-wavevector relation now has a band structure similar to a solid. As previously mentioned, the presence of strong interactions make this a difficult problem to solve and thus the exact band structure is unknown. Once the atoms have been loaded into the lattice their collective behaviour can be understood by studying the Bose-Hubbard Hamiltonian.

Bose-Hubbard model

In the simplest case of an infinite, uniform system, the Bose-Hubbard Hamiltonian is:

$$\mathcal{H} = -t \sum_{<i,j>} b_i^\dagger b_j + \frac{U}{2} \sum_i n_i(n_i - 1) - \mu \sum_i n_i \tag{2}$$

where $b_i^\dagger$ is the boson creation operator at site i, b_j is the boson annihilation operator at site j, t is the tunneling energy to a nearest neighboring site, $n_i = b_i^\dagger b_i$ is the number of atoms at site i, U is the on-site atom-atom interaction energy and μ is the chemical potential. The first term is related to the kinetic energy of atoms in the lattice and represents an atom tunneling from site j to site i at an energy cost to the system of t. For this term, the tight-binding approximation has been used to reduce the sum to nearest-neighbor lattice sites only, represented by the $< i, j >$ notation, so that t is equal for all terms. This is a good approximation for lattice depths of $5E_R$ and above. The second term is related to atom-atom interactions. Each pair of atoms on the same lattice site increases the energy of the system by U. The last term is simply the chemical potential of the system.

Deriving the Bose-Hubbard Hamiltonian

This model can be derived from the general form of a Hamiltonian using field operators which is given by:

$$\begin{aligned} \mathcal{H} = &\int \hat{\psi}^\dagger(\vec{r}) \left(\frac{\vec{P}^2}{2m} + V_0 \sum_{i=1}^{3} \sin^2(k_i x_i) \right) \hat{\psi}(\vec{r}) \mathrm{d}^3\vec{r} + \\ &\frac{1}{2} \iint \hat{\psi}^\dagger(\vec{r'}) \hat{\psi}^\dagger(\vec{r}) V(\vec{r'} - \vec{r}) \hat{\psi}(\vec{r}) \hat{\psi}(\vec{r'}) \mathrm{d}^3\vec{r'} \mathrm{d}^3\vec{r} - \mu N \end{aligned} \tag{3}$$

where $\hat{\psi}$ is the boson field operator, $\vec{P}$ is the momentum operator, $V(\vec{r'} - \vec{r})$ is a atom-atom interaction potential and N is the total number of particles. It is common to expand the boson field operators in terms a particular superposition of Bloch states called Wannier states. In this basis, the field operators are given by:

$$\hat{\psi}(\vec{r}) = \sum_i w_0(\vec{r} - \vec{r_i}) b_i \tag{4}$$

where $w_0(\vec{r}-\vec{r_i})$ is a Wannier state of the ground band centered at site i. Only the ground band is considered here due to the ultracold temperatures that the gases are cooled to before being loaded into the lattice.

Plugging in eq. 4 into the first term in eq. 3 and restricting the sum to nearest-neighbors, we find $t = -\int w_0^*(\vec{r}-\vec{r_i})\left(-\frac{\hbar^2}{2m}\vec{\nabla}^2 + V_0\sum_n \sin^2(k_n x_n)\right) w_0(\vec{r}-\vec{r_j})\mathrm{d}^3\vec{r}$ and hence obtain the first term of eq. 2. To evaluate the two-body interaction term, a pseudopotential approximation is used in the form of $V(\vec{r'}-\vec{r}) = U_0\delta(\vec{r'}-\vec{r})$. The constant of proportionality is determined from a scattering calculation utilizing the first-order Born approximation and it would be found that $U_0 = \frac{4\pi\hbar^2 a_s}{m}$ where a_s is the s-wave scattering length. This approximation to the interaction term is valid for a sufficiently dilute and cool gas. Substituting the definition of the field operators given by eq. 4 into eq. 3 and using boson commutation relations it is found that $U = \frac{4\pi\hbar^2 a_s}{m}\int |w_0(\vec{r})|^4 \mathrm{d}^3\vec{r}$. The last term is easily derived using $N = \sum_i n_i = \sum_i b_i^\dagger b_i$.

This system undergoes a quantum phase transition at zero temperature, the phase diagram for which will be shown later. In the limit that $U/t \to 0$, the system is a superfluid in the ground state with a wavefunction given by [1]:

$$|\Psi_{\mathrm{SF}}\rangle \propto \left(\sum_{i=1}^{M} b_i^\dagger\right)^N |0\rangle \tag{5}$$

where M is the number of lattice sites and N is the numbers of particles. Since it is energetically favorable for atoms to tunnel to other lattice sites in this regime, the above represents a delocalized state where each atom occupies every lattice site equally. Individual measurements would yield a random result for the number of particles on a single site. In the regime where $t/U \to 0$, it is energetically costly to have atom number fluctuations on lattice sites and the system is a Mott insulator where the ground state is [1]:

$$|\Psi_{\mathrm{MI}}\rangle = \left(\prod_{i=1}^{M} b_i^\dagger\right)|0\rangle. \tag{6}$$

The above represents a localized state where there is a single atom in every lattice site in order to minimize the energy of the system. It is important to note that the above is valid when the number of particles is equal to the number of lattice sites. For a particle number equal to an integer multiple, n, of lattice sites, the product in eq. 6 is raised to the exponent n. When this condition is not satisfied, the superfluid state persists even if the values of t/U and μ/U correspond to a Mott insulator region of the phase diagram.

Site-decoupled mean-field theory

A mean-field approximation can be used to simplify eq. 2 to generate a phase diagram [2]. The mean-field treatment involves ignoring fluctuations and considering the mean value of the boson creation and annihilation operators by making the approximation:

$$b_i^\dagger b_j \to \langle b_i^\dagger\rangle b_j + b_i^\dagger\langle b_j\rangle - \langle b_i^\dagger\rangle\langle b_j\rangle \tag{7}$$

to the first term in eq. 2. We define $\langle b_i \rangle = \psi$ and $\langle b_i^\dagger \rangle = \psi^*$ where ψ is the mean-field superfluid order parameter. Substituting eq. 7 into eq. 2, the mean-field Bose-Hubbard Hamiltonian is found to be:

$$\mathcal{H} = 6t \sum_i (|\psi|^2 - \psi b_i^\dagger - \psi^* b_i) + \frac{U}{2} \sum_i n_i(n_i - 1) - \mu \sum_i n_i. \tag{8}$$

As shown above, the mean field approximation from eq. 7 has produced a site-decoupled Hamiltonian. To generate a phase diagram from eq. 8, we consider the Hamiltonian on a single site i, use a Fock state of the number of atoms on that site as the basis and truncate the Hilbert space at some maximum number of atoms. The order parameter ψ is then varied to find the minimum possible value for the ground state energy at a fixed μ/U and t/U. Figure 1 is the phase diagram generated for an atom number truncation of 10. Figure 2 is a plot of the average atom number in the phase diagram. The Mott insulator phase occurs where the mean-field superfluid order parameter is zero and has integer values for the average occupation while the superfluid phases generally takes on non-interger values for the average atom number.

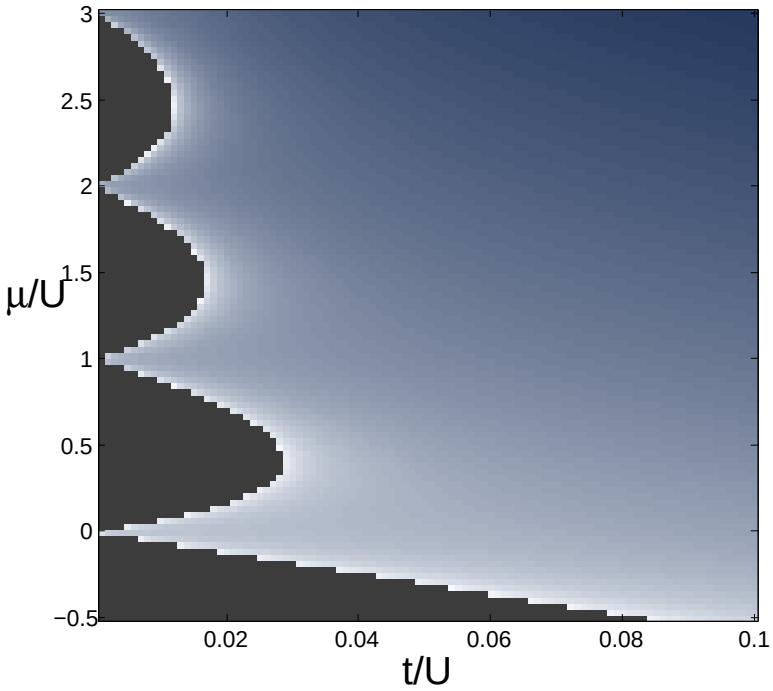

Figure 1: Plot of the mean-field superfluid order parameter of μ/U (y-axis) and t/U (x-axis) using the site-decoupled mean-field Hamiltonian. The grey lobes are where the order parameter is equal to zero indicating the presence of the Mott insulator phase. Outside of these lobes, the order parameter takes on a finite value and the superfluid phase exists.

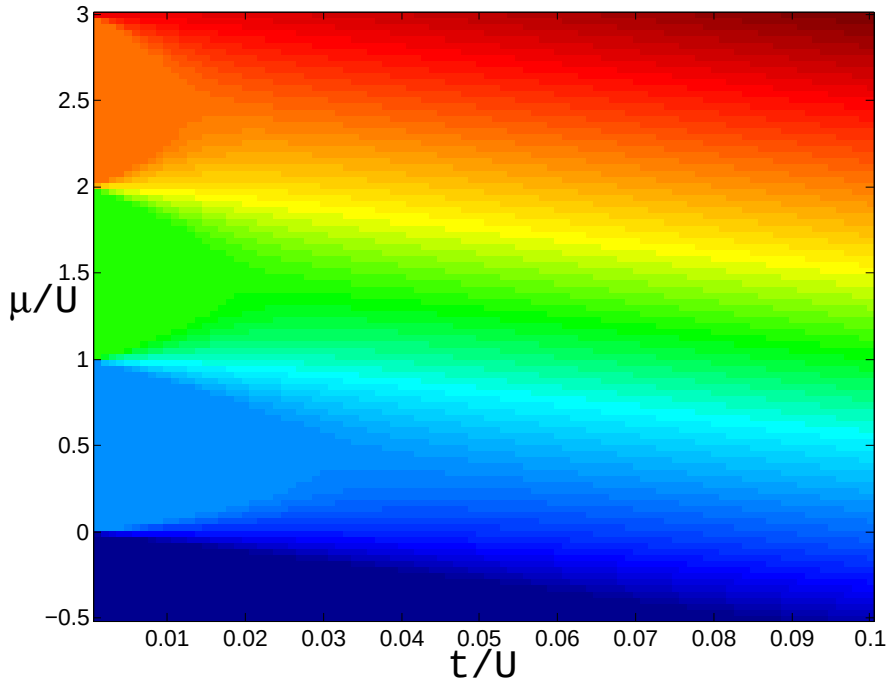

Figure 2: Plot of the average atom number on a single lattice site as a function of μ/U (y-axis) and t/U (x-axis) using the site-decoupled mean-field Hamiltonian. The dark blue section in the bottom left has an average occupation of 0 while the light blue, green (difficult to see) and orange lobes have average occupations of 1, 2 and 3 respectively. Away from these areas there is generally a non-interger value for the average occupation.

Experimental studies

In this section of the paper, experiments that first observed the emergent phases of this system, studied their properties and probed the excitation spectra will be discussed.

Observation of quantum phase transition and atomic Mott insulator properties

Greiner *et al.* were the first to study the superfluid to Mott insulator transiton in this system and probe some of its properties [3]. In their experiment, a pure Bose-Einstein condensate (BEC) of roughly 2×10^5 ^{87}Rb atoms was loaded from a magnetic trap into an 852 nm three-dimensional optical lattice by slowly ramping up the intensity of the lattice lasers to ensure the BEC always remains in the ground state of the combined potentials. The gas occupies about 15×10^4 lattice sites with an average filling of 2.5 atoms per site in the center of the lattice potential. The BEC was loaded into a shallow lattice such that the system was in the superfluid state. A superfluid has the property of macroscopic phase coherence and to verify its presence between lattice sites after the gas had been loaded into the optical lattice, the trapping potentials were snapped off and the gas was allowed to expand. Absorption images of the gas yielded a high-visibility interference pattern as shown in Figure 3 confirming the existence of phase coherence between lattice sites.

Increasing the lattice depth allows for the observation of the phase transition from the

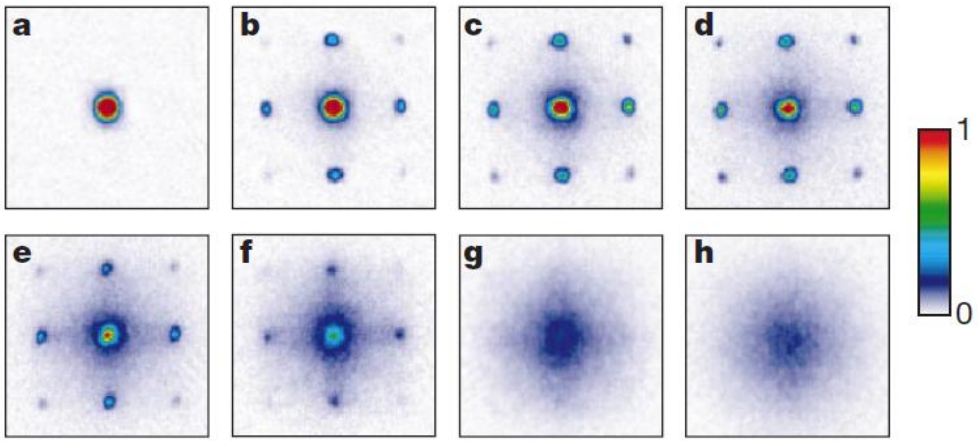

Figure 3: Absorption images of the atomic gas after the trapping potentials have been snapped off. For low lattice depths the gas is in a phase coherent state yielding an interference pattern. As the lattice depth is increased, the system enters a state where there is no phase coherence and the interference pattern has vanished. (Figure from [3])

superfluid state to a Mott insulator. The interaction energy U is an increasing function of the lattice depth V_0 while the tunneling energy t is a decreasing function as shown in Figure 4. Changing the lattice depth then translates into tuning the t/U ratio and allows access to different areas of the phase diagram of Figure 1. As shown in Figure 3, the visibility of the interference pattern degrades at larger values of the lattice depth and finally at a depth of $22E_R$ (Figure 3h), there is no recognizable interference pattern. The gas density profile is consistent with the idea that atoms want to occupy a single lattice site (or a single lattice site harboring an integer multiple of atoms) to minimize the energy of the system with no phase coherence between lattice sites. This absence of phase coherence between lattice sites is one of the properties of the Mott insulator state. Greiner *et al.* also demonstrate the reversibility of this process by showing that an interference pattern and hence phase coherence is restored after the lattice is ramped back down.

Another property of the Mott insulator state is the presence of a gap in the excitation spectrum. The energy gap E_g depends on the lattice depth and approaches U when the system is deep in the Mott insulator regime. For integer filling at small t/U, the lowest-lying excitation is taking an atom from a lattice site and putting it in a neighboring site at an energy cost U. This is a particle-hole excitation. Excitations were probed in the Mott insulator state through application of a potential gradient which causes tunneling to become a favorable process when the energy difference between two neighboring lattice sites equal U. To observe excitations, Greiner *et al.* relied on the effect that excitations in the Mott insulator phase have on the phase coherence of the superfluid state when the lattice is ramped back down. The result is a broadening of the interference pattern when the confining potentials are snapped off where the amount of broadening is used as a measure of the proximity to resonance for the excitation. Figure 5 shows data for excitations in the Mott insulator state where a gap can be seen for large lattice depths (Figure 5 e & f). The first resonance corresponds to particle-hole excitations and the second is hypothesized to be from a number of other processes.

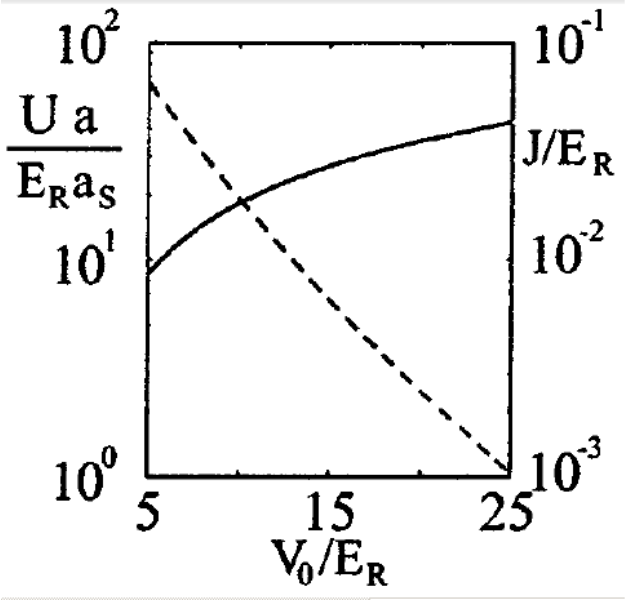

Figure 4: Plot of the atom-atom interaction energy U and the tunneling energy J versus the lattice depth V_0. The dotted line is the curve for J and the solid line is the curve for U. (Figure from [4])

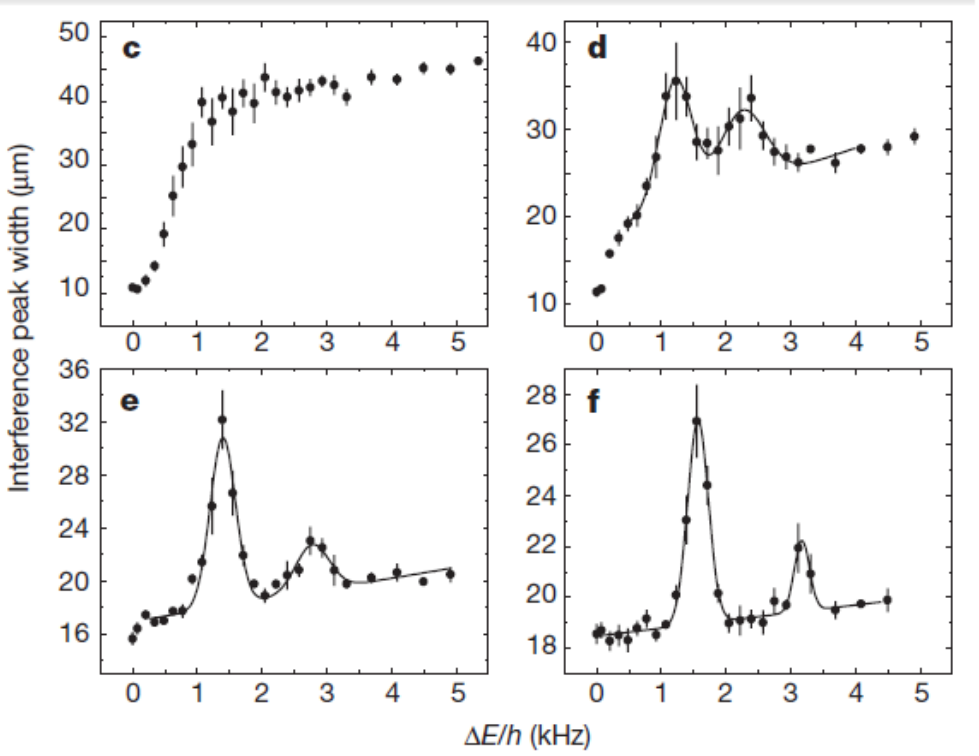

Figure 5: Data showing the excitation probably for various lattice depths. (Figure from [3])

This was pioneering work in creating the sub-field of quantum simulation of strongly-interacting solids in AMO physics. Though the authors claim that the energy gap and resonance in the excitation spectrum are direct evidence that they are in the Mott insulator

phase, the defining property of this phase is incompressibility, $\partial n/\partial \mu$[1]. While there is a wealth of indirect evidence here for the existence of these phases, Greiner *et al.* did not probe the compressibility of the Mott insulator phase or the presence of a critical velocity for the superfluid phase.

Observation of incompressible Mott insulator

Gemelke *et al.* used a BEC of ^{133}Cs atoms in a 2D optical lattice to experimentally verify the incompressibility of the Mott insulator phase [5]. In their setup, two pairs of orthogonal, counter-propagating 1064 nm laser beams in the horizontal(x-y) plane form the 2D optical lattice. Two more lasers beams are crossed at an angle of 15° and the resultant interference forms a lattice potential in the direction along the z-axis with 4 μm spacing between sites. The BEC was loaded into a single site of the vertical lattice and the lattice depth of the 2D lattice was ramped up to enter the Mott insulator phase. Absorption imaging along the z-direction was used to capture the atomic density profile in the x-y plane.

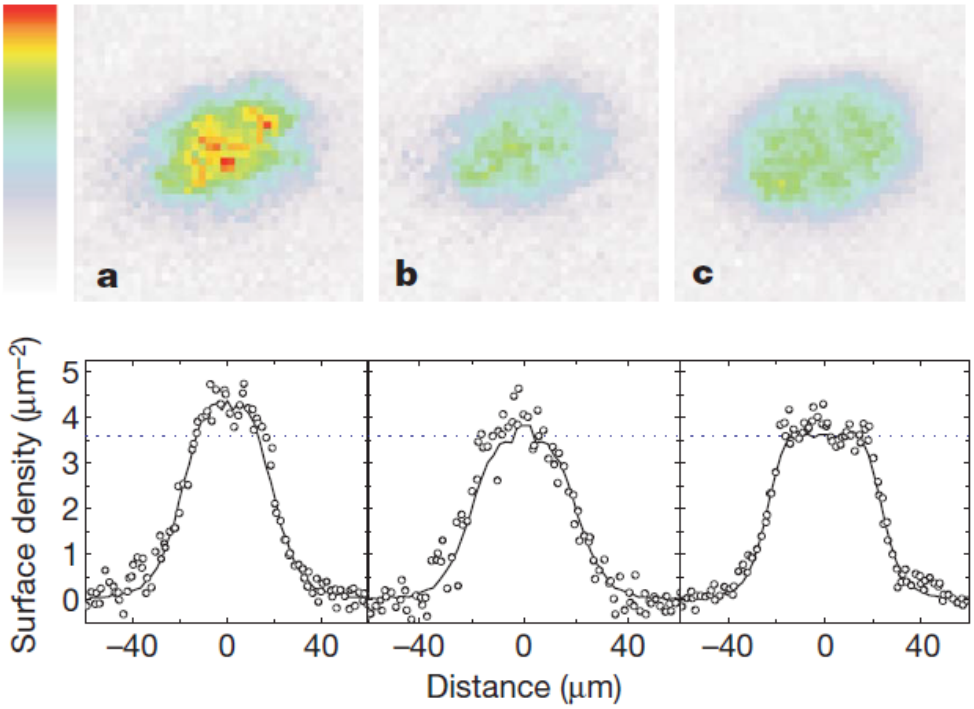

Figure 6: In situ absorption images of the lattice gas (top) and slices through the density profile (bottom) showing the gas density as a function of position. (Figure from [5])

At a lattice depth of 22 E_R, corresponding to a t/J value where the system is predicted to be in the Mott insulator phase, Gemelke *et al.* observe a flat density profile, shown in Figure 6 c, in the center of the trap. The atomic density in this region was measured to be 3.5(3) μm^{-2} (standard error in parentheses) which agrees well their theoretical calculation of 3.53 μm^{-2} for a filling of one atom per site. Additionally, Gemelke *et al.* found that $\kappa \propto \partial n/\partial r$ where κ is the compressibility and n is the atomic density. The compressibility near the trap center, shown in Figure 7 (red dots), was calculated and can be seen to be

consistent with zero. This experiment gives confidence in previous work claiming to observe the Mott insulator phase of bosonic atoms in an optical lattice.

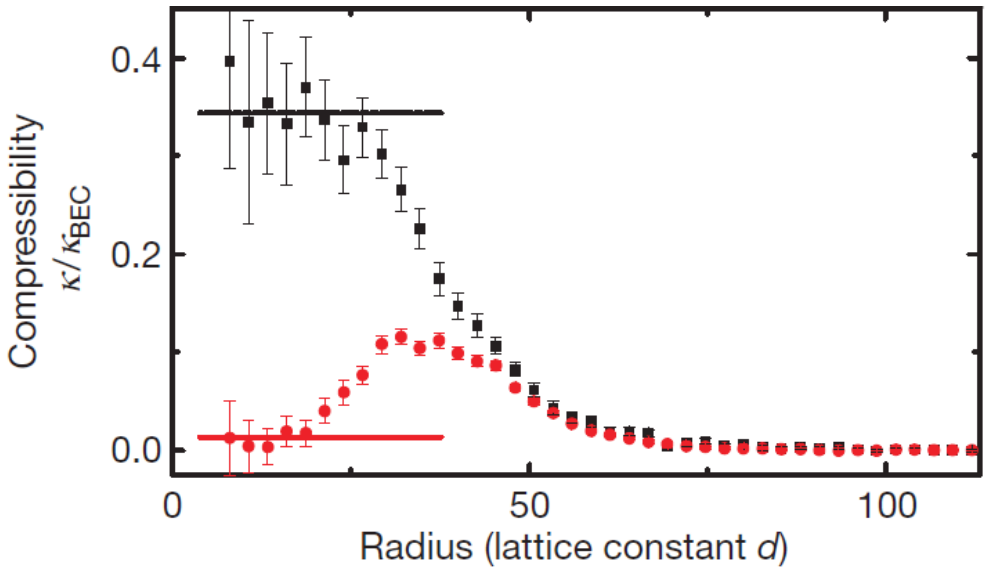

Figure 7: Compressibility of the lattice gas as a function of the distance from the center of the trap. The red dots are for a $22E_R$ lattice where a Mott insulator phase exists in the center. (Figure from [5])

Observation of critical momentum in a lattice superfluid

The approach taken by Mun *et al.* was to use a BEC of ^{87}Rb atoms in 3D optical lattice created by counter-propagating laser beams where one dimension had a frequency difference between the interfering beams forming the standing wave [6]. This frequency difference resulted in a moving lattice along this direction. The effect of the moving lattice is a state of the lattice gas with momentum $p = -m\lambda\delta f/2$ where λ is the lattice laser wavelength, δf is the frequency difference producing the moving lattice and m is the mass of the atom.

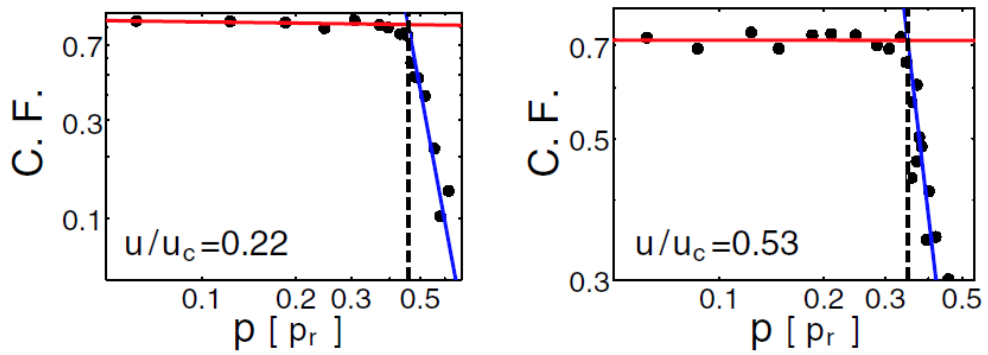

Figure 8: Plot of the condensate fraction versus the momentum imparted to the lattice gas for two values of U/t. (Figure from [6])

Once the moving lattice had perturbed the system, the external potentials were snapped

off and the gas was allowed to ballistically expand. The condensate fraction was then determined by measuring the broadening of the central peak of the resulting interference pattern. At a fixed ratio of U/t, the condensate fraction was measured as a function of the imparted momentum p and Figure 8 shows the data obtained for $U/t = 0.22$ and 0.53. The presence of a critical momentum is evident here in the rapid decrease of the condensate fraction. This procedure was repeated for various values of U/t and the data in Figure 9 was obtained. Taken together, Figures 8 and 9 provide direct evidence for the existence of a superfluid phase for small U/t.

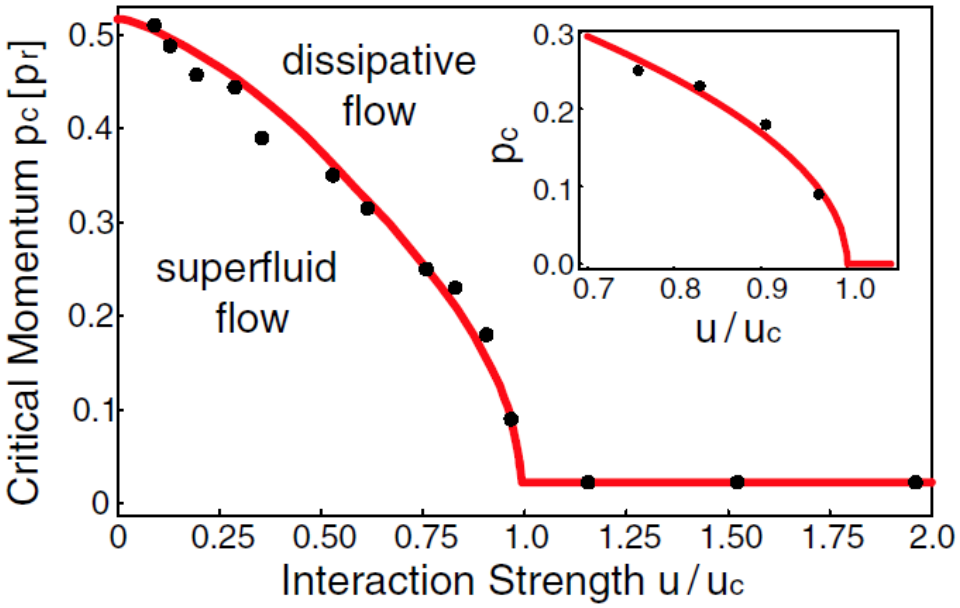

Figure 9: Plot of the critical momentum of the lattice gas as a function of the ratio of the atom-atom interaction energy to the tunneling energy U/t. (Figure from [6])

Conclusion

This paper has discussed the theory of bosonic atoms in an optical lattice and some important experiments that verified and probed the properties of the quantum phases of this system. The Bose-Hubbard Hamiltonian was derived from the general form of the Hamiltonian in the language of field operators and a mean-field approximation was used to obtain a site-decoupled Hamiltonian. From this, numerical calculations yielded the phase diagram and the average atom number in each part of the phase diagram. Various experiments were presented and discussed which observed the quantum phase transition, verified the defining properties of superfluid and Mott insulator phases and probed certain excitations of the system.

References

[1] I. Bloch, J. Dalibard, and W. Zwerger, Rev. Mod. Phys. **80**, 885 (2008).

[2] K. Sheshadri, H. R. Krishnamurthy, R. Pandit, and T. V. Ramakrishnan, Europhys. Lett. **22**, 257 (1983).

[3] M. Greiner, O. Mandel, T. Esslinger, T. W. Hansch, and I. Bloch, Nature **415**, 39 (2002).

[4] D. Jaksch, C. Bruder, J. I. Cirac, C. W. Gardiner, and P. Zoller, Phys. Rev. Lett. **81**, 3108 (1998).

[5] N. Gemelke, X. Zhang, C.-L. Hung, and C. Chin, Nature **460**, 995 (2009).

[6] J. Mun, P. Medley, G. K. Campbell, L. G. Marcassa, D. E. Pritchard, and W. Ketterle, Phys. Rev. Lett. **99**, 150604 (2007).